Int. J. Electrochem. Sci., 16 **(2021)** Article ID: 21069, doi: 10.20964/2021.06.35

International Journal of
ELECTROCHEMICAL
SCIENCE
www.electrochemsci.org

Synthesis of $Li_{1.05}M_xMn_{2-x}O_4$ (M = Co^{3+} and/or Cr^{3+}, x = 0.1 or 0.2) and their application as cathode materials for lithium-ion batteries

Xiuhua Zhang[1], Wanting Liu[1], Chenhao Zhao[1,], Shasha Yang[1], Baoping Zhang[2]*

[1] Fujian Provincial Key Laboratory of Clean Energy Materials, College of Chemistry & Materials, Longyan University, Fujian Longyan, China, 364000.
[2] Fujian Kinslithium Advanced Materials Company. Fujian Shanghang, China,
[*]E-mail: zhaochenhao123456@163.com

Received: 29 January 2021 / *Accepted:* 3 April 2021 / *Published:* 30 April 2021

Pristine $Li_{1.05}Mn_2O_4$ and its trivalent metal-substituted spinels of $Li_{1.05}M_xMn_{2-x}O_4$ (M = Co^{3+} and/or Cr^{3+}, x = 0.1 or 0.2) were synthesized by a simple citric acid-assisted sol-gel method. These trivalent metal ions can enter $Li_{1.05}Mn_2O_4$ crystal lattice and exert an influence on the crystal structure. Charge-discharge tests reveal that, in comparison with pristine $Li_{1.05}Mn_2O_4$, the cobalt- and/or chromium-doped spinels have relatively high capacity retentions over 100 cycles at a rate of 1 C. Taking co-doped $Li_{1.05}Co_{0.1}Cr_{0.1}Mn_{1.8}O_4$ as an example, it can maintain 93.2% of initial capacity after 100 charge-discharge cycles at 1 C at 55°C and can reach 80% capacity retention over 1000 cycles at a high rate of 5 C. Anyway, the enhanced cycle life of doped spinels can be attributed to the inhibitory effect of element doping on the Jahn-Teller distortion and manganese dissolution of pristine structures.

Keywords: Lithium manganese oxide; Li-ion battery; Trivalent metal ion; Element doping; Cyclability.

1. INTRODUCTION

Recently, Li-ion secondary batteries have been recognized as the most promising power source for their potential application in electric automobile (EV) and hybrid electric automobile (HEV) if high-rate cycling stability has been dramatically improved and the safety problem has been solved [1-3]. Insofar as the commonly used cathode material $LiCoO_2$ is concerned, it should not satisfy these demands owing to its high cost, serious environment pollution and safety issues. By comparison, the

alternative lithium manganese oxide spinel ($LiMn_2O_4$) deserves to be investigated because of abundant Mn source, relatively environmental friendly and better safety [4-6]. As for the cathode material $LiMn_2O_4$ during a charge-discharge process, the Jahn-Teller distortion of Mn^{3+} and the Mn dissolution into electrolyte should play an important role in shorting the cycle life especially at an elevated temperature [7-8]. Nowadays, surface coating and element doping have been successfully used to improve the cycling stability of $LiMn_2O_4$ [9-11]. As shown in literature reports, metal cations of Co^{3+}, Cr^{3+}, Zn^{2+}, Ti^{4+}, Fe^{3+}, Ni^{2+}, Gd^{3+}, Sm^{3+}, Ce^{4+}, Zr^{4+}, Er^{3+}, Mg^{2+} and Al^{3+} had been used for the partial substitution of Mn-ions in $LiMn_2O_4$ lattice structures, aiming at reducing the Mn^{3+} content in $LiMn_2O_4$ therein [12-24]. Considering the chemical valence of substituted elements, Co^{3+}, Cr^{3+} and Al^{3+} may be the most suitable ones due to their moderate ions radii and relatively high M-O bond energies. For example, commercial $LiMn_2O_4$ had an initial discharge capacity of 108.7 mAh g^{-1} at 0.2 C, which is not suitable for a long-term charge-discharge cycle. Interestingly, the modification of commercial $LiMn_2O_4$ using the co-doping of Co and Li (i.e., $Li_{1.05}Co_{0.1}Mn_{1.85}O_4$) could hold 86% of initial capacity after 1000 charge-discharge cycles at 200 mA g^{-1} [12]. Similarly, the Al-doped $LiMn_2O_4$ prepared through a polymer-pyrolysis route had capacity retention of 99.5% at 55°C after 50 charge-discharge cycles [24].

Aside from the surface coating and element doping, the crystallinity, morphology, particle size and size distribution can also exert a great influence on the cycling performance of spinel materials. The high crystallinity of spinel $LiMn_2O_4$ and element-doped ones means the stable framework of octahedron structure, which can probably decrease structure distortion, Mn dissolution and the transformation of spinel $LiMn_2O_4$ to rock salt phase Li_2MnO_3 during charge-discharge processes [25]. Also, spinel $LiMn_2O_4$ and element-doped ones with a nanosized dimension can provide a relatively short pathway for the diffusion of lithium ions [2,26-28]. In this paper, a simple citric acid-assisted sol-gel method was used to prepare pristine $Li_{1.05}Mn_2O_4$ and element-doped $Li_{1.05}M_xMn_{2-x}O_4$ (M = Co^{3+} and/or Cr^{3+}, x = 0.1 or 0.2). The structural and electrochemical properties of pristine $Li_{1.05}Mn_2O_4$ and M-doped $Li_{1.05}M_xMn_{2-x}O_4$ were investigated, concluding the enhanced electrochemical stability of pristine $Li_{1.05}Mn_2O_4$ through the doping of trivalent metal ions.

2. EXPERIMENTAL SECTIONS

2.1 Synthesis of materials

$Li_{1.05}M_xMn_{2-x}O_4$ (M = Co^{3+} and/or Cr^{3+}; x = 0.1 or 0.2) were prepared by a simple sol-gel route using citric acid a chelating agent. Typically, lithium acetate dehydrate ($CH_3COOLi{\cdot}2H_2O$), manganese acetate tetrahydrate $(CH_3COO)_2Mn{\cdot}4H_2O$) and the dopants of cobalt acetate tetrahydrate ($(CH_3COO)_2Co{\cdot}4H_2O$) and/or chromium nitrate nonahydrate ($Cr(NO_3)_3{\cdot}9H_2O$) were mixed together and dissolved into deionized water at a Li : (M+Mn) stoichiometric ratio of 1.05 : 2.00. Then, a certain amount of citric acid was added to reach a metal-ion : citric acid molar ratio of 9 : 4. And then, ammonia ($NH_3{\cdot}H_2O$ (25 ~ 28 wt%)) was dropwise used to adjust the solution pH at a value of 8.0 ~ 9.0. Thereafter, the as-prepared solution was heated to 80°C for the partial evaporation of water, and

the resulting viscous sol was dried at 140ºC for several hours to get a clear gel. Finally, the obtained gel was calcined at 750ºC for 6 h to produce the pristine spinel lithium manganese oxide (defined as $Li_{1.05}Mn_2O_4$ according to the stoichiometric ratio) and its element-doped $Li_{1.05}M_xMn_{2-x}O_4$. In order to investigate the influence of doped elements on the cycling stability of pristine spinel, $Li_{1.05}Mn_2O_4$ was also synthesized via the same sol-gel procedure as this described above.

2.2 Material characterization

The Au-coated samples of $Li_{1.05}M_xMn_{2-x}O_4$ were observed by JEOL JSM-7600F scanning electron microscope (SEM) with a field emission source and operated at an accelerate voltage of 15 KV. X-Ray diffraction patterns were carried out on a Rigaku D/max-2400 powder X-ray diffractormeter with Cu Kα radiation (40 KV, 40 mA). The 2θ range from 10 to 80° and scanning speed of 0.08º step per second were selected to analyze the effect of doped elements on crystal structures.

2.3 Electrochemical measurement

The obtained $Li_{1.05}M_xMn_{2-x}O_4$ was sufficiently mixed with acetylene black and polyvinylidene fluoride (PVDF) in a weight ratio of 8:1:1. Then, a rational amount of *N*-methyl pyrrolidone (NMP) was added into the mixture, and the resulting black slurry was pasted on aluminum foils, dried at 100ºC for about 10 h and then cut into circular discs (12 mm in diameter, 3-4 mg active material in weight). These disc-like pieces were dried under vacuum at 100ºC for at least 5 h, which were used working electrodes in 2032 coin cells. Lithium and aluminum foil were used as the counter electrodes and current collectors, respectively. Glass fibers (Whatman) were used as a separator, and the electrolyte was the commercial LBC 305-01 $LiPF_6$ solution (Shenzhen Xinzhoubang). The Li-ion battery cells were assembled in an argon-filled glove box. A galvanostatic cycling test of assembled coin-type cell was conducted on a LAND CT2001A system (Wuhan Landian) at different current densities and in the voltage range of 3.0–4.3 V (*vs.* Li^+/Li). Each sample is assembled three parallel coin cell for testing to ensure the accurate of results.

3. RESULTS AND DISCUSSION

At first, XRD characterization was used to determine the crystallographic structure and preferred orientation in the synthesized solid samples. For the XRD patterns of undoped and doped spinels (Fig. 1), all the diffraction peaks can be assigned and indexed using the standard data of pristine $LiMn_2O_4$ (JCPDS 35-0782). That is, the crystal phases of lithium-rich $Li_{1.05}M_xMn_{2-x}O_4$ (M = Co^{3+} and/or Cr^{3+}; x = 0.1 or 0.2) spinels belong to a single-issue, and no crystalline impurities can be detected. The inset in Fig. 1 is the magnified XRD diffraction peaks of (400) crystal plane, showing its peak shift with the effective doping of Co^{3+} and/or Cr^{3+} ions. Therefore, the doped trivalent metal ions come into the unit cell and lead to the crystal shrinkage of pristine $Li_{1.05}Mn_2O_4$ frameworks [29].

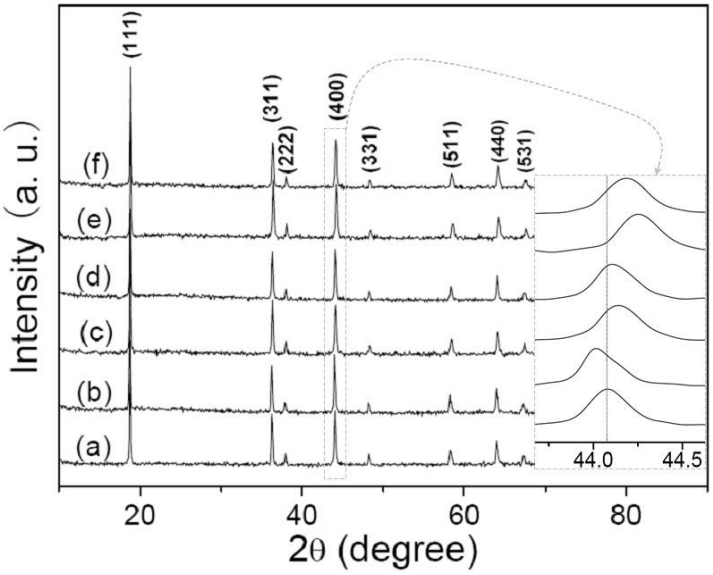

Figure 1. XRD patterns of $Li_{1.05}M_xMn_{2-x}O_4$: (a) x = 0, (b) M = Cr, x = 0.1, (c) M = Co, x = 0.1, (d) M = Cr, x = 0.2, (e) M = Co, x = 0.2, (g) M = Co + Cr, x = 0.2. Inset is the magnified (400) diffraction peaks around the 2θ position of 44.1°.

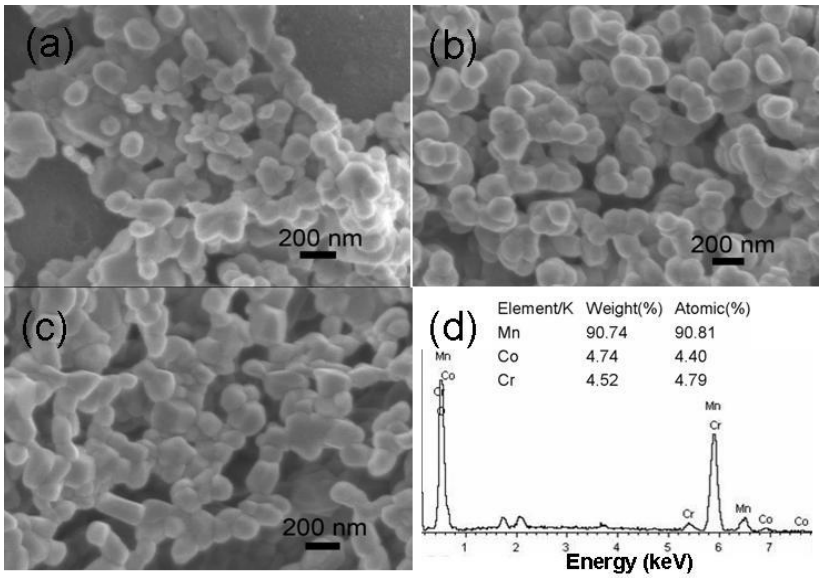

Figure 2. SEM images of $Li_{1.05}Mn_2O_4$ (a), $Li_{1.05}Co_{0.1}Mn_{1.9}O_4$ (b), $Li_{1.05}Co_{0.1}$ $Cr_{0.1}Mn_{1.8}O_4$ (c) samples, and energy dispersive spectrum analysis of a $Li_{1.05}Co_{0.1}Cr_{0.1}Mn_{1.8}O_4$ particle shows the Mn/Co/Cr atomic ratio of about 18/1/1 (d).

Fig. 2a–d are the SEM pictures of $Li_{1.05}Mn_2O_4$, $Li_{1.05}Co_{0.1}Mn_{1.9}O_4$ and $Li_{1.05}Co_{0.1}Cr_{0.1}Mn_{1.8}O_4$, showing clear edges and corners of nanoparticles with a polydisperse size distribution of 100 ~ 400 nm. In general, nanofabricated spinels should provide a relatively short pathway for the extraction and insertion of lithium ions but means the relatively high possibility for Mn dissolution during charge-

discharge processes. The primary motivation of sol-gel syntheses deals with the precise control of chemical composition for small quantities of dopants and the nanofabrication of spinel materials [30, 31]. Herein, it should be pointed out that the agglomeration of nanoparticles is due to the sintering behavior of nanosized materials during thermal treatment of gel-like precursors (Fig.2a-c). The energy dispersive spectrum of $Li_{1.05}Co_{0.1}Cr_{0.1}Mn_{1.8}O_4$ presents that the atomic ratio of Cr/Co/Mn is closed to the corresponding raw materials ratio of 1.0/1.0/1.8 (Fig. 2d).

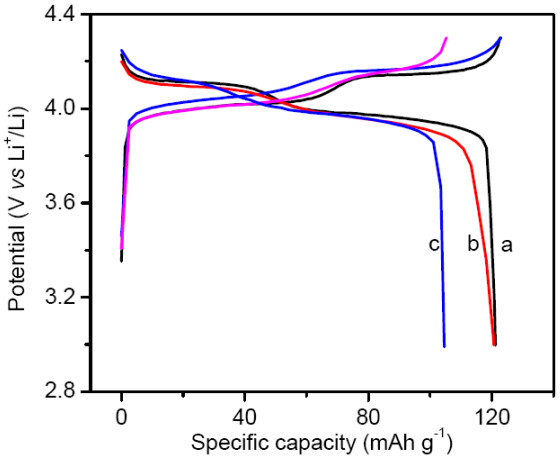

Figure 3. The typical 2nd cycle charge-discharge curves of $Li_{1.05}Mn_2O_4$ (a), $Li_{1.05}Co_{0.1}Mn_{1.9}O_4$ (b), and $Li_{1.05}Co_{0.1}Cr_{0.1}Mn_{1.8}O_4$ (c) electrodes.

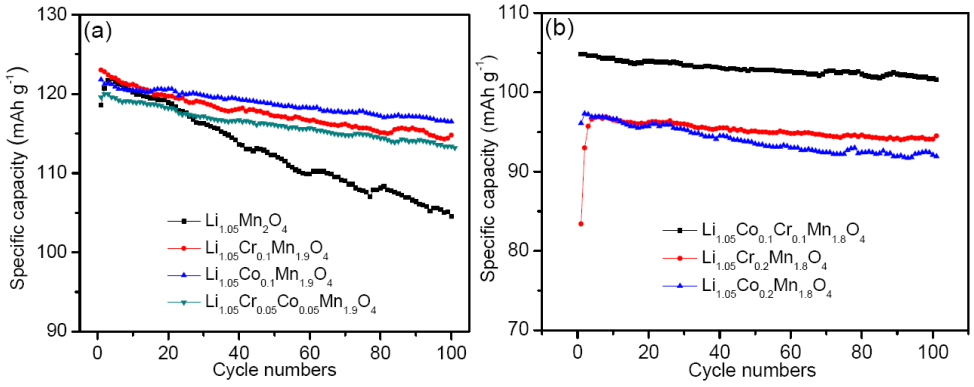

Figure 4. The plots of $Li_{1.05}M_xMn_{2-x}O_4$ discharge capacity against cycle numbers at a rate of 1 C at room temperature: (a), x = 0.0 or 0.1; (b), x = 0.2.

Typically, the galvanostatic cycling results of pristine $Li_{1.05}Mn_2O_4$, single-doped $Li_{1.05}M_{0.1}Mn_{1.9}O_4$ and the co-doped $Li_{1.05}Co_{0.1}Cr_{0.1}Mn_{1.8}O_4$ spinels, operated within the voltage range of 3.0 - 4.3 V at 1 C (i.e., 148 mA g^{-1}) at room temperature, were shown in Fig.3. Each sample exhibits a charging plateau around ~3.95 V, a discharging plateau around ~4.05 V and an intersection point at

the middle. These indicate a weak electrochemical polarization of obtained materials as rechargeable battery cathodes. Furthermore, the pristine, single- and co-doped spinels display a decreasing trend of discharge capacity in order, which can be explained by the increasing amount of substituted trivalent metal ions [32].

The cycling stabilities of $Li_{1.05}M_xMn_{2-x}O_4$ cathode materials with a relatively low and high substitution degree of elements were shown in Fig. 4a and 4b, respectively. At room temperature, pristine $Li_{1.05}Mn_2O_4$ has the discharge capacity retention of 85.7 % after 100 cycles, while the retention values of single- and co-doped $Li_{1.05}M_{0.1}Mn_{1.9}O_4$ are as high as 93% and 95% under the same conditions (Fig. 4a). It should be pointed out that the curve fluctuation of a discharge capacity-cycle number plot, not the decreasing trend, is due to the day-and-night temperature difference. If the lattice structure of $Li_{1.05}Mn_2O_4$ could be well maintained with the doping of trivalent metal ions, the average valence of transition metal ions in $Li_{1.05}M_xMn_{2-x}O_4$ should be about 3.5 [23]. That is, the relatively good cyclability of $Li_{1.05}M_{0.1}Mn_{1.9}O_4$ may be due to the relatively high average value of Mn valance therein (Fig. 4a).

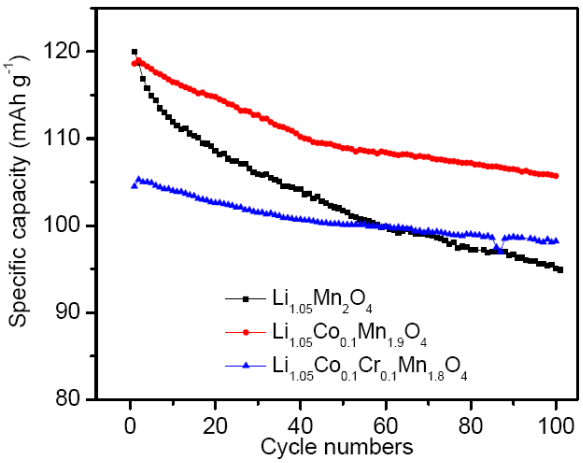

Figure 5. The plots of $Li_{1.05}M_xMn_{2-x}O_4$ discharge capacity against cycle numbers at a rate of 1 C at 55°C: x = 0.0, 0.1 or 0.2.

Table 1. Galvanostatic charge-discharge results of spinel $Li_{1.05}M_xMn_{2-x}O_4$ in Li-ion batteries operated at different temperatures (i.e., room temperature RT and 55ºC).

Cathode active material	Initial capacity (±3) mAh g-1 (RT)	100th capacity (±3) mAh g^{-1} (RT)	Retention % (RT)	Initial capacity (±3) mAh g^{-1} (55°C)	100th capacity (±3) mAh g^{-1} (55°C)	Retention % (55°C)
$Li_{1.05}Mn_2O_4$	121.9	104.5	85.7	120.0	95.1	79.2
$Li_{1.05}Co_{0.1}Mn_{1.9}O_4$	121.8	116.5	95.6	119.0	105.7	88.8
$Li_{1.05}Co_{0.1}Cr_{0.1}Mn_{1.8}O_4$	104.8	101.7	97.0	105.3	98.2	93.2

At the substitution degree of 0.1, the cycling stability of co-doped $Li_{1.05}Co_{0.05}Cr_{0.05}Mn_{1.9}O_4$ is higher than that of $Li_{1.05}Cr_{0.1}Mn_{1.9}O_4$ but is lower than that of $Li_{1.05}Co_{0.1}Mn_{1.9}O_4$ (Fig. 4a). That is, Co substitution seems to be good for the retention of initial capacity at a relatively low substitution degree. Also, according to the XRD patterns shown in Fig. 1, spinel materials with the Cr substitution degree of 0.1 have relatively little lattice shrinkages of an octahedron unit [33]. Therefore, the Co and Cr co-doped samples of $Li_{1.05}Co_{0.1}Cr_{0.1}Mn_{1.8}O_4$ could explain the cyclability improvement through a possible synergistic effectiveness. At the substitution degree of 0.2, the cycling stability of $Li_{1.05}Co_{0.1}Cr_{0.1}Mn_{1.8}O_4$ is the best, maintaining 97.0% of initial capacity at room temperature (Fig. 4b).

Generally, Mn dissolution should be enhanced at a relatively high temperature, which seriously affects the cycling performances of spinel materials. In order to study the influence of operating temperature, the electrochemical measurements of Li-Mn-O cathode material were carried out at 55°C, shown in Fig. 5. The detailed information was listed in Tab. 1, it should be pointed out that the error of electrochemical values is about ±3 mAh g^{-1} based on the mass error of working electrodes. For example, the undoped one has the highest initial capacity of 120 mAh g^{-1} at 55°C, which fades fast to a value of 95 mAh g^{-1} after 100 charge-discharge cycles. Interestingly, the co-doped material of $Li_{1.05}Co_{0.1}Cr_{0.1}Mn_{1.8}O_4$ can maintain 93.2% of initial capacity under the exact same conditions in assembled cells. This further proves that the cycling stability of Li-Mn-O spinels can be improved by the single- or co-doped substitution of trivalent Co and Cr ions.

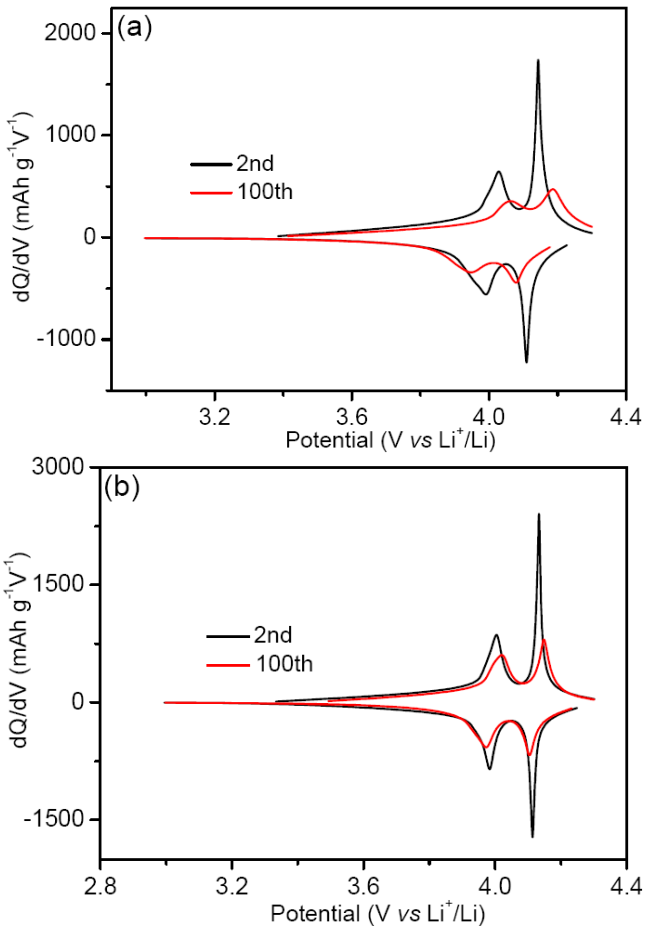

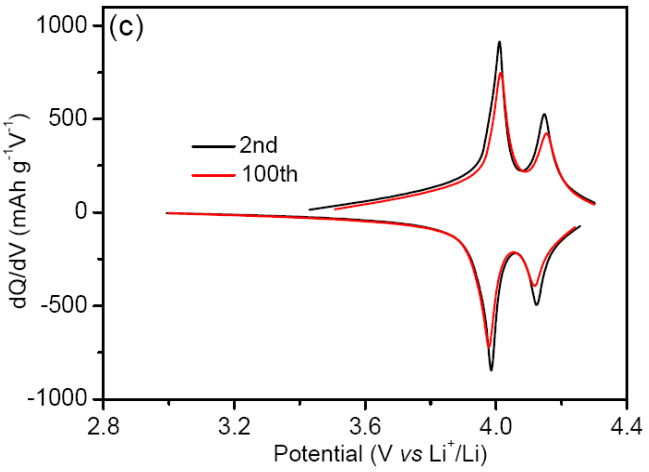

Figure 6. The plots of dQ/dV against V for the 2nd and 100th cycle at current density of 1C at 55ºC: $Li_{1.05}Mn_2O_4$ (a), $Li_{1.05}Co_{0.1}Mn_{1.9}O_4$ (b) and $Li_{1.05}Co_{0.1}Cr_{0.1}Mn_{1.8}O_4$ (c).

In consideration of the structural properties of $Li_{1.05}M_xMn_{2-x}O_4$ with the single- and co-doped elements, it is necessary to analyze the charge-discharge curves as the plots of dQ/dV versus V, where V is the cell's voltage and Q is the charge that flows.

As for the comparative $Li_{1.05}Mn_2O_4$, $Li_{1.05}Co_{0.1}Mn_{1.9}O_4$ and $Li_{1.05}Co_{0.1}Cr_{0.1}Mn_{1.8}O_4$, the analyzed results of the 2nd and 100th cycles operated at current density of 1C at 55ºC are showed in Fig. 6. In comparison with the 2nd cycle, the corresponding charge-discharge curve at the 100th cycle shows a discharge voltage of dQ/dV peaks shifts at the relatively low value. Also by comparison, there is a more shift for pristine $Li_{1.05}Mn_2O_4$ (Fig. 6a), a middle shift for single-doped $Li_{1.05}Co_{0.1}Mn_{1.9}O_4$ (Fig. 6b) and a less shift for co-doped $Li_{1.05}Co_{0.1}Cr_{0.1}Mn_{1.8}O_4$ (Fig. 6c). These suggest a relatively strong interaction between intercalated atoms with the structural host of co-doped $Li_{1.05}Co_{0.1}Cr_{0.1}Mn_{1.8}O_4$ [34 35].

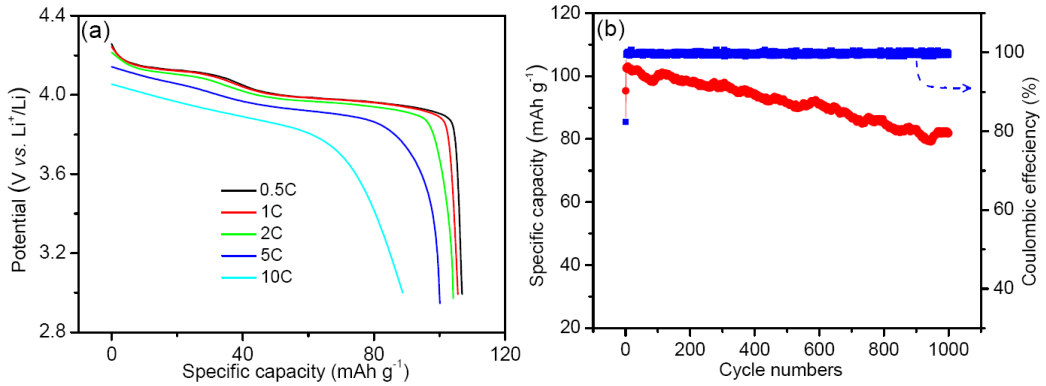

Figure 7. Rate-capability (a) and Long-term cycling stability (b) of $Li_{1.05}Co_{0.1}Cr_{0.1}Mn_{1.8}O_4$ electrode at a high current density of 5C.

Table 2. Cycle performance data of $LiMn_2O_4$ samples modified by different methods

Samples	Preparation route	Cycle temperature (℃)	Capacity retention(cycle number, cycling rate)	Initial reversible discharge capacity (cycling rate) ($mAh\ g^{-1}$)
$Li_{1.05}Co_{0.10}Mn_{1.85}O_4$	Solid state reaction[12]	RT	94(300 , 2C), 86(1000, 2C)	81.3(0.2C)
		55	85（100, 1C）	
Li_3PO_4-coated $LiMn_2O_4$	Sol-gel route[37]	55	85（100, 1C）	114.2(1C)
$LiCoO_2$-coated $LiMn_2O_4$	Micro-emulsion process[38]	RT	95（100, 0.5mA cm^{-2})	113(0.5mA cm^{-2})
		55	85(80, 0.5mA cm^{-2})	
$LiMn_2O_4$/Ag (Ag5wt%)	One-step ombustion[39]	RT	93.7（100, 0.5C）	110(2C)
		55	88.1（100, 2C） 71.5（100, 5C）	
3 wt% ZrO_2-coated $LiMn_2O_4$	One-time sintering[40]	RT	90.1(400, 1C)	118.8（0.2C）
		55	88.9(150, 1C)	
$Li_{1.05}Co_{0.1}Cr_{0.1}Mn_{1.8}O_4$(This work)	Sol-gel route	RT	97(100, 1C)	105(1C) 103.1(2C)
		55	93.2(100, 1C) 80(1000, 5C)	

Aside from the electrochemical durability at a relatively high temperature, high-rate capability and cyclability are also the key factors to explore the potential application of element-doped spinels. At a charge-discharge rate of 2 C, 5 C and 10 C, the discharge capacities of $Li_{1.05}Co_{0.1}Cr_{0.1}Mn_{1.8}O_4$ are 103.1, 99.7 and 88.9 mAh g-1, shown in Fig. 7a. Under the same experimental conditions, undoped $Li_{1.05}Mn_2O_4$ electrode merely acquires a discharge capacity of 98.8 and 44.4 mAh g-1 at 2 C and 5 C, respectively. As shown in Fig.7b, the discharge capacity of $Li_{1.05}Co_{0.1}Cr_{0.1}Mn_{1.8}O_4$ electrode at 5 C decreases slowly and almost linearly, and it can surprisingly maintain 80% of maximum capacity after 1000 cycles. To the best of our knowledge, the long-term and high-rate cycling stability of $Li_{1.05}Co_{0.1}Cr_{0.1}Mn_{1.8}O_4$ may satisfy its potential application as rechargeable batteries in EV and HEV energy storage sources, which is excellent in comparison with the ever reports [20, 36]. The cycling performance of series $LiMn_2O_4$ has been summarized in Table 2[12,36-40].In comparison, the co-doped $Li_{1.05}Co_{0.1}Cr_{0.1}Mn_{1.8}O_4$ electrode demonstrates substantively cycling stability, especially at an elevated temperature of 55 ℃.

4. CONCLUSION

In summary, a simple sol-gel method was successfully used to prepare single- and/or co-doped spinels of $Li_{1.05}M_xMn_{2-x}O_4$ ($M = Co^{3+}$ and/or Cr^{3+}, x = 0.1 or 0.2). The substitution of trivalent metal ions can enter pristine $Li_{1.05}Mn_2O_4$ crystal lattice, decrease the dissolution of Mn and improve the structural stability of resulting spinels. These induce the enhanced cycling stability of lithium

manganese oxide electrodes during charge-discharge processes. As for the co-doped $Li_{1.05}Co_{0.1}Cr_{0.1}Mn_{1.8}O_4$ electrode, it can surprisingly maintain 93.2 % of initial capacity at 1 C over 100 cycles at 55°C and 80 % of initial capacity at a high rate of 5 C after 1000 cycles at room temperature, which can be attributed to synergistic effect of doped cobalt and chromium elements.

ACKNOWLEDGEMENT
The financial support from the Innovation Train Program of College Student (201911312051), New Materials Research Center of Shanghang County and Education Research Program (Science and Technology) of Fujian province (JAT200598)

Reference

1. K.Tang, Y.F.Xue, G.Teobaldi, L.M.Liu, *Nanoscale Horiz.*, 5 (2020)1453-1466 .
2. S. Chen, Z. Chen, C. B. Cao, Electrochimica Acta, 199 (2016) 51–58.
3. J. M. Tarascon, N. Recham, M. Armand, J. N. Chotard and P. Barpanda, *Chem. Mater.*, 22 (2010),724-739.
4. B. L. Ellis, K. T. Lee and L. F. Nazar, *Chem. Mater.,* 22 (2010) 691-714.
5. J. B. Goodenough and Y. Kim, *Chem. Mater.,* 22 (2010) 587-603.
6. J. Y. Luo, H. M. Xiong, Y. Y. Xia, *J. Phys. Chem. C,* 112 (2008) 12051-12057.
7. S. Lim and J. Cho, *Electrochem. Chem.,* 10 (2008) 1478-1481.
8. D. Arumugam and G. P. Kalaignan, *J. Electroanaly. Chem.,* 624 (2008) 197-204.
9. Z. H. Chen, Y. Qin, K. Amine and Y. K. Sun, *J. Mater. Chem.,* 20 (2010) 7074-7095.
10. A. Banerjee, B. Ziv, S. Luski , D. Aurbach , & I. C. Halalay, J. Power Sources, 341(2017) 457–465.
11. P. Pang, Z. Wang, X. Tan, Y. Deng, J. Nan, Z. Xing & H. Li, Electrochim Acta, 327 (2019) 135018 .
12. C. Y. Wang, S. G. Lu, S. R. Kan and J. Pang, *J. Power Sources,* 189 (2009) 607-610.
13. J. M. Amarilla, R. M. Rojas, F. Pico and L. Pascual, *J. Power Sources,* 174 (2007) 1212-1217.
14. D. Arumugam, G. P. Kalaignan, K. Vediappan and C. W. Lee, *Electrochim. Acta,* 55 (2010) 8439-8444.
15. L. L. Xiong, Y. L. Xu, T. Tao, X. F. Du and J. B. Li, *J. Mater. Chem.,* 21 (2011) 4937-4944.
16. P. Singh, A. Sil, M. Nath and S. Ray, *Phy. B,* 405 (2010) 649-654.
17. H. M. Wu, J. P. Tu, X. T. Chen and X. B. Zhao, *J. Solid State Electrochem.,* 11 (2007) 173-176.
18. D. Arumugam, G. P. Kalaignan and P. Manisankar, *Solid State Ionics,* 179 (2008) 580-586.
19. S. R. K. Balaji, M. Mutharasu and S. Shanmugan, *Ionics,* 16 (2010) 351-360.
20. M. Helan, L. J. Berchmans, R. Ravisankar and V. M. Shanmugam, *Mater. Res. Innov.,* 15 (2011) 130-134.
21. X. H. Liu, J. Q. Wang, J. Y. Zhang and S. R. Yang, *J. Mater. Sci.,* 17 (2006) 865-870.
22. H. W. Liu, L. Song and K. L. Zhang, *Inorg. Mater.,* 41 (2005) 646-649.
23. K. S. Lee, H. J. Bang, S. T. Myung, K. Amine and Y. K. Sun, *J. Power Sources,* 174 (2007) 726-729.
24. L. F. Xiao, Y. Q. Zhao, Y. Y. Yan, Y. L. Cao, X. P. Ai and H. X. Yang, *Electrochim. Acta,* 54 (2008) 545-550.
25. Y. K. Sun, Y. S. Lee and M. Yoshio, *Mater. Lett.,* 56 (2002) 418-423.
26. Y. G. Wang, Y. Q. Li, P. He and H. S. Zhou, *Nanoscale,* 2 (2010) 1294-1305.
27. Y. Yang, C. Xie, R. Ruffo, H. L. Peng and Y. Cui, *Nano Lett.,* 9 (2009)4109-4114.

28. E. Hosono, T. Kudo, I. Honma and H. S. Zhou, *Nano Lett.,* 9 (2009)1045-1051.
29. Z. D. Peng, Q. L. Jiang, K. Du, W. G. Wang, G. R. Hu and Y. X. Liu, *J. Alloy Compd.,* 493 (2010) 640-644.
30. R. Thirunakarana, A. Sivashanmugama, S, Gopukumara and R. Rajalakshmib, *J. Power Sources,* 187 (2009) 565-574.
31. B. L. He, W. J. Zhou, Y. Y. Liang, B. S. Juan and H. L. Li, *J. Colloid Interface Sci.,* 300 (2006) 633-639.
32. S. L. Zhao, H. Y. Chen, J. B. Wen and D. X. Li, *J. Alloy Compd.,* 474 (2009) 473-476.
33. Y. C. Su, Q. F. Zou, Y. W. Wang, P. Yu and J. Y. Liu,*Mater. Chem. Phys.,* 84 (2004) 302-307.
34. K. S. Lee, S. T. Myung, H. J. Bang, S. Chung and Y. K. Sun, *Electrochim. Acta*, 52 (2007) 5201-5206.
35. D. Q. Liu, Z. Z. He and X. Q. Liu,*Mater. Lett.*, 61 (2007) 4703-4706.
36. D. Arumugam and G. P. Kalaignan,*Electrochim. Acta,* 55 (2010) 8709-8716.
37. Li, X. Yang, R. Cheng, B. Hao, Q. Xu, H. Yang, J. & Qian, Y. *Mater. Lett,,* 66(2012) 168-171.
38. Z. Liu, H. Wang, L. Fang., J. Y. Lee, and L. M.Gan. *J. Power Sources*, 104(2002) 101-107..
39. R.Jiang, C. Cui, H. Ma, H. Ma and T. Chen. *J.Electroanaly. Chem.,* 744(2015) 69-76.
40. G. Li, X. Chen, Y. Liu, Y. Chen. and W. Yang. RSC Adv., 30(2018) 16753-16761.